



spectral method. This method in addition, allows establishing the qualitative composition of hydrocarbons in the analyzed samples. So, it was found that more than 80 wt. % of fuel oil in the composition is vacuum distillate and heavier fractions.

The proton spectrum of fuel oil from AGPP contains  $^1\text{H}$  signals of paraffinic, naphthenic and aromatic compounds, which are the main components of the mixture. Methyl proton signals from saturated hydrocarbons were detected as a broadened singlet at 0.90 ppm. High-intensity signal with a chemical shift of 1.28 ppm indicates a significant content of protons of methylene groups of aliphatic cyclic and acyclic hydrocarbons. The highest-frequency signals ( $\delta = 6.97\text{--}7.76$  ppm) indicate the presence of monoaromatic compounds and condensed aromatic rings in the fuel oil. Signals of methyl protons of saturated hydrocarbons (HC) are noted as a broadened singlet at 0.90 ppm. A small amount of  $\text{CH}_3$  groups was noted in the  $\alpha$ -position to the aromatic ring ( $\delta = 2.30\text{--}2.63$  ppm). In the range of 2.70–4.50 ppm probably the resonance of protons of the  $\text{CH}_2$  and  $\text{CH}$  groups in the  $\alpha$ -position of aromatic compounds [17, 35–40].

## RESULTS AND DISCUSSIONS

It was found that the optimum sizes of active parts of the catalyst are 40–50 nm. Specific surface of the catalyst calculated according to full isotherms of low-temperature adsorption of nitrogen by BET method makes  $12.6\text{ m}^2/\text{g}$ . Integral volume of pores is  $0.57\text{ ml/g}$ . SEM images of isolated aluminosilicate microspheres extracted from fly ash of TPP are shown in the Figure-1.

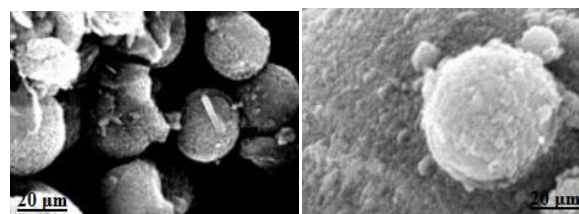


**Figure-1.** SEM images of aluminosilicate microspheres extracted from fly ash of TPP-2, Almaty.

The chemical composition (Table-2) is represented by oxides of aluminum, silicon, iron, calcium and titanium (ca. 95 wt. %).

**Table-2.** The elemental and chemical composition of aluminosilicate microspheres (cenospheres), % wt.

Sample	$\text{Al}_2\text{O}_3$	$\text{SiO}_2$	$\text{CaO}$	$\text{TiO}_2$	$\text{Fe}_2\text{O}_3$	$\text{Na}_2\text{O}$	S	P	SrO	ZrO
Initial	26.5	59.4	2.14	1.193	5.52	0.82	0.187	0.599	0.041	0.053
1	26.6	57.49	1.16	1.07	4.93	3.59	1.58	0.467	0.043	0.053
2	25.37	56.77	1.82	1.10	5.67	3.75	1.86	0.536	0.045	0.055
3	25.84	58.3	1.38	1.08	5.59	3.30	2.74	0.599	0.07	0.06
4	25.75	57.6	0.93	1.12	5.61	2.85	3.64	0.54	0.06	0.05
5	25.90	57.3	0.03	1.13	5.60	1.77	5.78	0.49	0.052	-

### Purification of Gas Emissions from Sulphur Dioxide

To study the kinetics of oxidation of sulfur dioxide by oxygen in stationary conditions in the presence of modified cenospheres as a catalyst,  $\text{Na}_2\text{SO}_3$  was used as a source of  $\text{SO}_2$ , inasmuch as under the experiment conditions at  $\text{pH} = 10\text{--}12$  in an aqueous solution  $\text{SO}_2$  is in the form of  $\text{SO}_3^{2-}$  and the reaction (1) was actually studied:



The main results of the study of microspherical catalysts of oxidation of sodium sulfite by oxygen are summarized in the Table-3. From the data of the Table-3 it follows that the degree of conversion and the ratio of the process depend on the concentrations of components of the system  $\text{Na}_2\text{SO}_3\text{--Al--O--Si--Fe--H}_2\text{SO}_4\text{--H}_2\text{O}$ . In optimal conditions, the  $\text{Na}_2\text{SO}_3$  rate conversion reaches 100 %, the maximum oxygen absorption rate reaches 6.8 ml/min.

Figure-2 shows the conversion curves in coordinates  $W_{\text{O}_2} = f(Q_{\text{O}_2})$ , where  $W_{\text{O}_2}$  is the rate of oxygen absorption in mol/l·min;  $Q_{\text{O}_2}$  is the amount of absorbed oxygen in mol/l, as well as potentiometric curves in

coordinates  $\varphi(Q_{\text{O}_2})$ , where  $\varphi(V)$  is the redox potential of the platinum electrode in relation to the calomel half-element. In most cases, the  $\text{Na}_2\text{SO}_3$  oxidation rate dependence on the initial concentrations of the components has extreme nature. The initial redox potential of the  $\text{Na}_2\text{SO}_3\text{--Al--O--Si--Fe--MX--H}_2\text{SO}_4\text{--H}_2\text{O}$  system, where MX is a modifying component, is placed in the range 0.8–0.45 V, with  $d\varphi/C_{\text{Na}_2\text{SO}_3} < 0$ , passing through the maximum,  $d\varphi/dT > 0$ . These results allow to suppose that the redox-determinative pair in this case is  $\text{Fe}^{3+}/\text{Fe}^{2+}$ . Conversion curves in coordinates  $W_{\text{O}_2} = f(Q_{\text{O}_2})$  (Figures-2a, c) and potentiometric curves in coordinates  $\varphi = f(Q_{\text{O}_2})$  (Figure-2b) show that with the  $\text{Na}_2\text{SO}_3$  introduction into the redox system, the potential sharply shifted to the cathode region by 0.5–0.25V, and oxygen absorption starts immediately. The potential jump depends on the components correlation in the system. In the course of the experiment, the potential returns to the anode region, in optimal conditions - to the initial value, which indicates that the reaction products do not change the structure and composition of the catalyst and it works in a sustained way under these conditions. In these conditions, the potential